

A Robust H_∞ Control Approach for Blood Glucose Regulation in Type-1 Diabetes

L. Cassany* D. Gucik-Derigny* J. Cieslak* D. Henry*
R. Franco** A. Ferreira de Loza***,**** H. Ríos***,****
L. Olçomendy* A. Pirog* Y. Bornat* S. Renaud*
B. Catargi†

* *IMS Lab, University of Bordeaux, Bordeaux INP, CNRS (UMR 5218), 351 cours de la liberation, 33405 Talence, France.*

** *Tecnológico Nacional de México/I.T. La Laguna, División de Estudios de Posgrado de Investigación, C.P. 27000, Torreón Coahuila, México.*

*** *Instituto Politécnico Nacional-CITEDI, C.P. 22435, Tijuana, Baja California, México.*

**** *Cátedras CONACYT, C.P. 03940, Ciudad de México, México.*

† *Bordeaux Hospitals, Diabetology Unit, F-33000, Bordeaux, France.*

Abstract: The paper addresses the design of a H_∞ closed-loop dedicated to Blood Glucose (BG) regulation for patients affected by Type-1 Diabetes Mellitus (T1DM). The closed-loop setup is standard, *i.e.* the H_∞ feedback controller uses the information provided by a subcutaneous sensor to drive an insulin pump but as opposed to current existing solutions, it is proposed to assess the capabilities of a H_∞ controller to be designed in a patient-independent way. For that purpose, the design is performed on a family of linear models in order to tackle the variability of a cohort of T1DM patients. Worst-case performance and robust margins are next computed with the help of the H_∞/μ -analysis theory. The solution is finally assessed on the adult cohort of the high-fidelity UVA/Padova benchmark (v3.2), accepted by the US Food and Drug Administration (FDA) as a substitute for pre-clinical testing of control strategies.

Keywords: Blood Glucose Regulation, H_∞ control, Type 1 Diabetes Mellitus

1. INTRODUCTION

Type-1 diabetes Mellitus (T1DM) is an autoimmune disease associated with β pancreatic cell death, which delivers the insulin necessary for Blood Glucose (BG) control. To avoid hyperglycemia ($BG > 180\text{mg/dL}$) and hypoglycemia ($BG < 70\text{mg/dL}$), the design of partially automated devices known as Artificial Pancreas (AP), receives a growing attention for non-intrusive care for T1DM patients (Rodbard, 2016). From the different elements that make up a AP, the controller is in charge of processing the information delivered by a Continuous Glucose Monitor (CGM) sensor to maintain the BG level in the so-called normoglycaemia range ($70\text{mg/dL} < BG < 180\text{mg/dL}$) by acting on an insulin pump. The present work focuses on an alternative control design for BG regulation.

From a recent survey (Quiroz, 2019), the available control design methodologies include those based on sliding mode theory (Gallardo Hernández et al., 2013; Franco et al., 2021), Proportional-Integral-Derivative (PID) (Steil et al., 2011; Olçomendy et al., 2020), Linear Parameter-Varying (LPV) tools, (Kovács, 2017; Colmegna et al., 2021) and Model Predictive Control (MPC) (Del Favero et al., 2014; Gondhalekar et al., 2018) to name a few. In this paper, it is proposed to focus on works developed in a H_∞ framework. The work (Kienitz and Yoneyama, 1993) addressed for

the first time the BG regulation with H_∞ techniques to manage the considerable amount of model uncertainty. This work has been followed by (Parker et al., 2000) where a sensitivity analysis provides the three-parameter set having the most significant effect on insulin and glucose dynamics. The BG regulation has been next formulated as a tracking one in (Ruiz-Velázquez et al., 2004) where a Glucose Tolerance Curve (GTC) of healthy patients has been used as reference model. Next, it is possible to find several robust H_∞ controllers (Femat et al., 2009; Flores-Gutiérrez et al., 2011; Mandal et al., 2014) that have been designed for an intravenous BG measurement. Motivated by the possibility of finding distinct frequency responses for a T1DM patient cohort, an attempt has been made to individualize the controller design in (Hernández-Medina et al., 2018). However, the price to pay is an increased complexity to tune the controller for clinicians and patients, which can not be always compliant with medical protocols.

The goal of this paper is to propose an alternative to the previous H_∞ control solutions. More precisely, it proposes to design a unique feedback controller able to be robust to the physiological characteristic variability of an adult patient cohort. Using the powerful H_∞ controller design theory applied to clinical issues, individual tuning is not required anymore. From the nonlinear model proposed in

(Dalla Man et al., 2014; Messori et al., 2018), a family of uncertain linear time invariant (LTI) models is established to capture physiological variabilities (Cassany et al., 2021). Here, we investigate a robust H_∞ controller designed with the H_∞ mixed-sensitivity approach (Zhou and Doyle, 1998). An analysis is then performed to highlight the robust margins and worst-case performance by means of the H_∞/μ -analysis theory. The proposed solution is finally assessed in the nonlinear UVA/Padova simulator (v3.2) developed under a Matlab/Simulink environment. This simulator is the first (and currently only) T1DM model accepted by the U.S. Food and Drug Administration (FDA) as a substitute for pre-clinical testing of new treatment strategies for T1DM. It provides a realistic simulation environment to assess new control algorithms under high-fidelity conditions with a representative cohort of T1DM patients (eleven adults in this study case).

The paper is organized as follows: section 2 provides some preliminaries to tackle the H_∞ mixed-sensitivity approach. Section 3 deals with the application to T1DM issue and Section 4 presents the simulation results in the T1DM simulator.

Notations: s is the Laplace transform variable and for a linear state space model (A, B, C, D) , $P(s)$ (or simply P) is its associated Laplace transform. The notation $P(s) : \begin{bmatrix} A & B \\ C & D \end{bmatrix}$ is used in the paper. $P(s)$ is assumed to belong to $\mathbb{R}H_\infty$, defined as the real rational functions set, with $\|P\|_\infty = \sup_\omega \bar{\sigma}(P(j\omega)) < \infty$, where $\bar{\sigma}(P)$ denotes the maximum singular value of the matrix P . For some matrices N and $M = \begin{pmatrix} M_{11} & M_{12} \\ M_{21} & M_{22} \end{pmatrix}$, the upper Linear Fractional Transformation (LFT) is defined as $\mathcal{F}_u(M, N) = M_{22} + M_{21}N(I - M_{11}N)^{-1}M_{12}$. Given $M(s)$ and a block-diagonal operator $\Delta \in \mathbf{\Delta} : \|\Delta\|_\infty \leq 1$ that gathers all uncertainties of a given model in a so-called $M - \Delta$ structure, the structured singular value $\mu_\Delta(M(j\omega)) : \omega \in \mathbb{R}_+$ is equal to zero if no Δ makes $I - M(j\omega)\Delta$ singular. Otherwise $\mu_\Delta(M(j\omega)) = [\min_{\Delta \in \mathbf{\Delta}} \{\bar{\sigma}(\Delta) : \det(I - M(j\omega)\Delta) = 0\}]^{-1}$.

2. MATERIAL BACKGROUNDS OF H_∞ CONTROL

The goal of the H_∞ mixed-sensitivity control approach is to design a controller $K(s)$ that stabilizes the closed-loop system and achieve some required robustness and control performance (Kwakernaak, 1993; Zhou and Doyle, 1998). The performance are also expressed as constraints $W_1(s)$ and $W_2(s)$, see Fig. 1 for an illustration. They act as frequency weighting functions that allow to shape the sensitivity function $S(s) = (I + G(s)K(s))^{-1}$ and the control sensitivity function $R(s) = K(s)S(s)$ in the H_∞ -norm sense, i.e.

$$\bar{\sigma}(S(j\omega)) \leq |W_1^{-1}(j\omega)|, \quad \forall \omega \in \mathbb{R}_+, \quad (1)$$

$$\bar{\sigma}(R(j\omega)) \leq |W_2^{-1}(j\omega)|, \quad \forall \omega \in \mathbb{R}_+, \quad (2)$$

where $W_1(s)$ is used to ensure that the controller $K(s)$ meets some performance criteria such as time response, static error, module margin, etc. $W_2(s)$ is used to enforce the control signal u to meet required specifications such as noise amplification, avoiding control saturation, minimising the energy $\|u\|_2$.

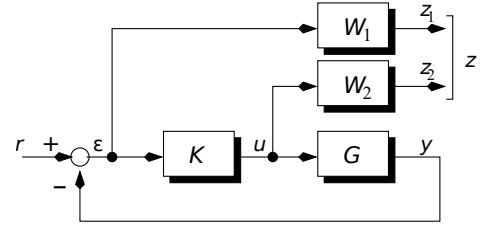


Fig. 1. Block diagram of the mixed sensitivity approach. Merging (1) and (2) into a unique H_∞ constraint leads to

$$\|T_{zr}\|_\infty \leq 1, \quad \text{with } T_{zr}(s) = \begin{pmatrix} W_1(s)S(s) \\ W_2(s)R(s) \end{pmatrix} \quad (3)$$

where $T_{zr}(s)$ is the transfer from r to z . However, this is a sub-optimal problem to solve of (1) and (2) since, at a given frequency ω^* ,

$$\bar{\sigma} \begin{pmatrix} W_1(j\omega^*)S(j\omega^*) \\ W_2(j\omega^*)R(j\omega^*) \end{pmatrix} \leq \sqrt{2} \max(\bar{\sigma}(W_1(j\omega^*)S(j\omega^*)), \bar{\sigma}(W_2(j\omega^*)R(j\omega^*)))$$

by virtue of the singular value properties. This means that the solution of (3) will be close to $\sqrt{2}$ of the optimal solution.

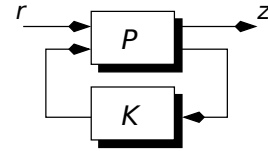


Fig. 2. The H_∞ standard problem.

From (3), the block diagram of Fig. 1 can be transformed into the diagram depicted in Fig. 2, referred as the standard H_∞ problem. In that context, $P(s)$ is the augmented system that contains $W_1(s)$ and $W_2(s)$. The controller design problem can then be stated as follows. Given a real rational transfer matrix $P(s)$ and a space \mathcal{K} of real rational transfer matrices $K(s)$ called the controller space, the computation of an optimal solution $K^*(s) \in \mathcal{K}$ leads to the solving of the following optimization problem

$$\begin{aligned} & \text{minimize } \gamma \\ & \text{subject to } K(s) \text{ stabilizes } P(s) \text{ internally} \\ & K(s) \in \mathcal{K}, \|T_{zr}\|_\infty \leq \gamma \end{aligned} \quad (4)$$

If the optimal value γ^* is strictly less than 1, then (1) and (2) hold. This is a sufficient condition for K^* , since a parameter γ^* such that $1 \leq \gamma^* \leq \sqrt{2}$ may correspond to a viable controller because of (4). That is why, practically, (1) and (2) are *a posteriori* verified by plotting the so-called “sigma-plot”. As we shall see from (4), the choice of the controller space $\bar{\mathcal{K}}$ is the key for a proper understanding of the problem. Let us define the following notations:

$$P(s) : \begin{bmatrix} A & B_1 & B_2 \\ C_1 & D_{11} & D_{12} \\ C_2 & D_{21} & D_{22} \end{bmatrix} \quad K(s) : \begin{bmatrix} A_K & B_K \\ C_K & D_K \end{bmatrix} \quad (5)$$

with $A \in \mathbb{R}^{n \times n}$, $B_2 \in \mathbb{R}^{n \times n_u}$, $C_2 \in \mathbb{R}^{n_y \times n}$ and $A_k \in \mathbb{R}^{n_k \times n_k}$. The so-called “full-order controller” solution behaves to the solutions within of the space

$$\bar{\mathcal{K}} = \{K(s) : K(s) \text{ has the form (5) with } n_k = n\} \quad (6)$$

which is a convex space. Thus, finding a solution within $\bar{\mathcal{K}}$ may be done by using an optimization algorithm.

In (Gahinet and Apkarian, 1994), the authors propose an algorithm by reducing (4) to a semi definite programming problem. This technique is retained in this paper.

3. APPLICATION TO THE T1DM ISSUE

The work presented in this paper follows a preliminary one reported in (Cassany et al., 2021) which introduces a way to model T1DM patients by means of a family of linear models. This family of linear models is used to cover the cohort dynamics of adult patients with different physiological characteristics (age, weight, etc.), see section II.A of (Cassany et al., 2021). Here, the focus is made on the integration of uncertainties in this cohort modelling step by using Linear Fractional Transformation (LFT). Then, the control problem is formulated in H_∞ framework and addressed through an equivalent LMI problem solving. The controller design is next addressed with the choice of the weighting functions. Finally, a discussion is proposed to evaluate the nominal performance, the robust stability and the *a posteriori* worst-case analysis.

3.1 Modelling issues

The method reported in (Cassany et al., 2021) enables to model the T1DM patient's dynamics as a family of linear models. The key element relies on finding an equivalent linear model of the nonlinear model presented in (Dalla Man et al., 2014), for judiciously chosen set points. To proceed, the method considers time horizon $[0, T]$ divided into subintervals such that $0 = t_0 < \dots < t_k < t_n = T$. The set $\lambda = (\lambda_0, \dots, \lambda_k, \lambda_n)$ is defined such as:

$$\begin{cases} \lambda_0 \in [t_0, \frac{t_1}{2}], \\ \lambda_k \in [\frac{t_k + t_{k-1}}{2}, \frac{t_{k+1} + t_k}{2}] \text{ for } 1 \leq k < n, \\ \lambda_n \in [\frac{t_n + t_{n-1}}{2}, t_n], \end{cases} \quad (7)$$

On each subinterval, $t \in \lambda_k$ for $k \in \{0, \dots, n\}$, k linear models associated to patient index $i \in \{1, \dots, 11\}$, are built so that

$$\begin{cases} \dot{x}^i(t) = A(\rho)_k^i x^i(t) + B(\rho)_k^i u^i(t) \\ y^i(t) = C(\rho)_k^i x^i(t) \end{cases} \quad (8)$$

$x(t) \in \mathbb{R}^{13}$, $u(t) \in \mathbb{R}^2$, $y(t) \in \mathbb{R}$ are respectively the model state, input and output vectors, with the matrices $A_k^i \in \mathbb{R}^{13 \times 13}$, $B_k^i \in \mathbb{R}^{13 \times 2}$ and $C_k^i \in \mathbb{R}^{1 \times 13}$. A key feature in this model is that the 4th and 13th states are the BG's and the subcutaneous (SC) glucose concentrations, respectively. Since it is assumed that a CGM equips the patients, we have $y^i(t) = x_{13}^i(t)$.

Two sources of uncertainty are considered in this work: the patient's characteristics (like weight, age, etc.) and the dynamics of BG diffusion to the SC space, where the electrode of the CGM is inserted. These uncertainties are also captured by the vector ρ that enters in (8).

With regards to the patient's characteristics, they are modelled using the so-called non-structured multiplicative uncertainty form, that is reformulated using the LFT formalism. Such a model is derived from (8) as follows:

$$\begin{aligned} Gb_k^i(s) &= C_4(\rho)_k^i (sI - A(\rho)_k^i)^{-1} B(\rho)_k^i s \quad \forall i, k \\ &= Gb_0(s)(1 + W_{\text{unc}}(s)\Delta_b(s)) = \mathcal{F}_u(P_b(s), \Delta_b(s)) \end{aligned} \quad (9)$$

where $C_4(\rho)$ is used to refer to the 4th state.

In (9), Δ_b is normalized (i.e. $\|\Delta_b\|_\infty \leq 1$), which implies

$$|W_{\text{unc}}(j\omega)| \geq |Gb_k^i(j\omega)/Gb_0(j\omega) - 1|, \quad \forall i, k, \omega, \quad (10)$$

This latest equation offers a constructive solution to determine the couple (Gb_0, W_{unc}) . In particular, the optimal solution $(Gb_0^*, W_{\text{unc}}^*)$ in the sense of the smallest conservative LFT, is constructed such that $\|W_{\text{unc}}\|_\infty$ is minimal. This optimization problem leads to the results given in Fig. 3, where W_{unc}^* is found of order 11. However, choosing a simple constant for $W_{\text{unc}} \approx 0.92$ leads the LFT $\mathcal{F}_u(P_b(s), \Delta_b(s))$ to be less complex, with a little extra conservativeness. The maximum gap between the optimal solution W_{unc}^* and $W_{\text{unc}} \approx 0.92$ is about 1.5dB. Towards this end, the constant solution is retained in this paper.

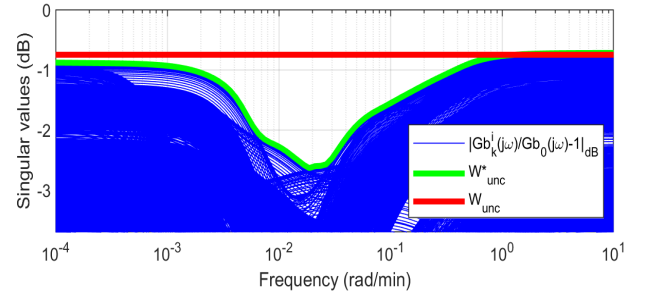


Fig. 3. Frequency behaviour of $|G_k^i(j\omega)/G_0(j\omega) - 1|$ (blue), $W_{\text{unc}}^*(j\omega)$ (green) and W_{unc} (red).

With regards to the dynamics of the BG's diffusion to the SC space, a deeper analysis of the model (8) reveals that it is reflected by a gain variation of the transfer between the 4th and the 13th state. Such a variation can be easily captured by a LFT so that

$$G_{sc_k}^i(s) = \mathcal{F}_u(P_{sc}(s), \Delta_{sc}), \quad \forall i, k \quad \Delta_{sc} \in \mathbb{R} : |\Delta_{sc}| \leq 1 \quad (11)$$

3.2 Control problem formulation

We are now ready to formulate the control design problem: in accordance with the theory explained in Section 2, let's consider the mixed-sensitivity H_∞ control setup given in Fig. 4 with the LFTs (9) and (11). The goal is to compute the controller $K(s)$ so that

$$\|\mathcal{F}_u(\mathcal{F}_l(P(s), K(s)), \Delta)\|_\infty < 1, \quad \Delta \in \mathbb{R}^2 : \|\Delta\|_\infty \leq 1, \quad (12)$$

where $\Delta = \text{diag}(\Delta_b, \Delta_{SC})$. In Fig. 4, G_{DAC} refers to the digital-analog converter considered here as a delay of $T/2$, $T = 1$ min (a Pade approximation of first order is used here). $P(s)$ is obtained from the different transfers occurring in Fig. 4.left, using linear-fractional algebra:

$$\begin{pmatrix} z_{\Delta_b} \\ z_{\Delta_{sc}} \\ z_1 \\ z_2 \\ \varepsilon_{sc} \end{pmatrix} = \begin{pmatrix} P_{b11} & 0 & 0 & P_{b12} \\ P_{sc12}P_{b21} & P_{sc11} & 0 & P_{sc12}G_{\text{DAC}}P_{b22} \\ -W_1P_{b21} & 0 & W_1 & -W_1G_{\text{DAC}}P_{b22} \\ 0 & 0 & 0 & W_2 \\ -P_{sc22}P_{b21} & -P_{sc21} & 1 & -P_{sc22}G_{\text{DAC}}P_{b22} \end{pmatrix} \begin{pmatrix} w_{\Delta_b} \\ w_{\Delta_{sc}} \\ r \\ u \end{pmatrix}, \quad (13)$$

with $P_b = \left(\begin{array}{c|c} P_{b11} & P_{b12} \\ \hline P_{b21} & P_{b22} \end{array} \right)$, $P_{sc} = \left(\begin{array}{c|c} P_{sc11} & P_{sc12} \\ \hline P_{sc21} & P_{sc22} \end{array} \right)$: $P_{b_{ij}}, P_{sc_{ij}} \in \mathbb{C}^1 \quad \forall i, j$.

The originality of the proposed control problem formulation as opposed to those addressed in (Femat et al., 2009; Flores-Gutiérrez et al., 2011; Mandal et al., 2014),

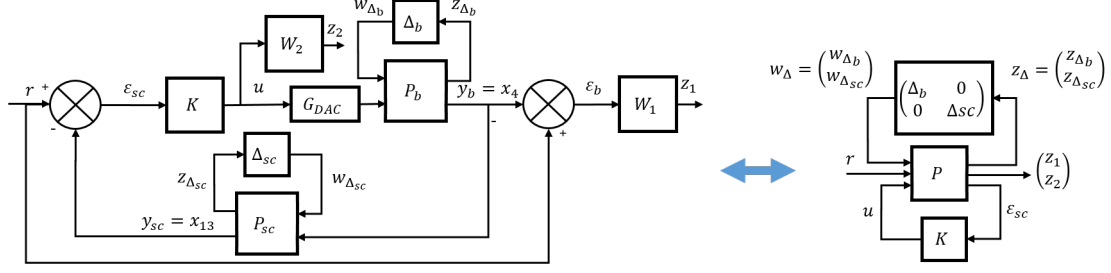


Fig. 4. Mixed sensitivity approach for the T1DM issue.

relies on the fact that the control objectives are set on the BG's concentration (i.e. the 4th state of (8)) without having a direct measurement of it, the measure being the SC's glucose concentration (i.e. the 13th state of (8)). This particular facet motivates the choice to capture the SC's dynamics variability in the LFT (11).

3.3 Design of the controller $K(s)$

Following the methodology explained in Section 2, the problem now turns out to be the definition of the weighting functions W_1 and W_2 that will constraint the sensitivity and control sensitivity functions S and R defined according to:

$$S(s, \Delta) = [1 + K(s)G_{\text{DAC}}\mathcal{F}_u(P_b(s), \Delta_b) (\mathcal{F}_u(P_{sc}(s), \Delta_{sc}) - 1)] [1 + G_{\text{DAC}}\mathcal{F}_u(P_b(s), \Delta_b)\mathcal{F}_u(P_{sc}(s), \Delta_{sc})K(s)]^{-1} \quad (14)$$

$$R(s, \Delta) = K(s) [1 + \mathcal{F}_u(P_b(s), \Delta_b)\mathcal{F}_u(P_{sc}(s), \Delta_{sc})G_{\text{DAC}}K(s)]^{-1} \quad (15)$$

To proceed, let $W_1^{-1}(s)$ be defined as

$$W_1^{-1}(s) = g_1 \left(\frac{s + \omega_l}{s + \omega_{c1}} \right), \quad (16)$$

where ω_{c1} is the minimal bandwidth required for the closed-loop, ω_l is a frequency introduced to make $W_1(s)$ invertible and can be chosen arbitrarily. The lower ω_l is, the lower will be the gain of $W_1^{-1}(s)$ (and $S(s)$) in low frequencies, resulting in a small static tracking error. g_1 is the gain of $W_1^{-1}(s)$ in high frequencies and represents the constraint on the gain margin. For our application, ω_{c1} is set to 0.03 rad/min, ω_l to 10^{-7} rad/min and g_1 to 5.6 (≈ 15 dB).

With regards to $W_2(s)$, let $W_2^{-1}(s)$ be defined as

$$W_2^{-1}(s) = g_2 \left(\frac{1/\omega_h s + 1}{1/\omega_{c2} s + 1} \right), \quad (17)$$

where ω_h is chosen such that invertibility property of $W_2(s)$ is guaranteed and the constraint $\omega_h \gg \omega_{c2}$ holds. Since the sampling rate in the T1DM simulator is set to $T = 1$ min, ω_h does not need to be set higher than $\omega_h = \pi/T$, according to Nyquist–Shannon theorem. The term $g_2/(1/\omega_{c2}s + 1)$ is a low-pass filter in which an adequate choice of (g_2, ω_{c2}) is achieved to minimize the control signal energy. Here, we have $g_2 = 17.7$ (≈ 25 dB) and $\omega_{c2} = 5\omega_{c1}$.

By such a choice, it can be verified that the control specifications have been fixed according to:

- S.1) A minimum gain margin of 5dB for $S(s, \Delta)$.

- S.2) A maximum bandwidth of $\omega_c = 0.03$ rad/min for $R(s, \Delta)$.

Practical considerations: There exist two main practical approaches to calculate $K(s)$ that solves (12). *i)* The first one consists in using the small gain theorem with (13). The result is known to be conservative since the small gain theorem does not consider neither the diagonal structure of Δ nor its nature. The μ -based criteria that are discussed in the next section are then used to assess the conservativeness of $K(s)$. *ii)* The second approach consists in choosing a judicious numerical value Δ_0 for Δ and to compute the controller $K(s)$ over $\mathcal{F}_u(P, \Delta_0)$. Because we have no guarantee that the resulting controller is able to satisfy the specifications for all Δ , μ analysis is required. However, we know that if we want to have a chance to succeed, γ in (4) must not be close to 1.

In this work, the second approach is used with $\Delta_0 = 0$, i.e. the design of $K(s)$ is done using the nominal model associated to $P(s)$. *i)* Using Matlab, (9) and (11) are first computed in order to assess their respective uncertainties. *ii)* After choosing the weighting functions in (16) and (17), one can build the interconnection matrix $P(s)$ in (13). *iii)* The problem described in (4) is finally solved using the SDP technique proposed in (Gahinet and Apkarian, 1994). The result leads to an optimal value for γ , found to be $\gamma^* \approx 0.48$.

3.4 Performance and worst-case analysis

As previously explained, μ -based criteria are now computed to assess robust stability and worst-case performance. The goal is to check if Specifications S.1 and S.2 are met. Due to space limitation, the reader is invited to refer to (Packard and Doyle, 1993) and (Zhou and Doyle, 1998) for the necessary background about μ concepts.

To proceed, $S(s, \Delta)$ is put in a LFT manner, i.e. $S(s, \Delta) = \mathcal{F}_u(M, \Delta) : \varepsilon_b(s) = S(s, \Delta)r(s)$ where M is partitioned according to the input/output signals ε_b/r and $w_\Delta = \Delta z_\Delta$ leading to $M = \begin{pmatrix} M_{11}(s) & M_{12}(s) \\ M_{21}(s) & M_{22}(s) \end{pmatrix}$.

Robust stability margins: The robust stability margin is defined as $m_r = [\max_{\omega \in \Omega} \mu_\Delta(M_{11}(j\omega))]^{-1}$. If $m_r > 1$, robust stability is achieved for all $\Delta \in \mathbf{\Delta} : \|\Delta\|_\infty \leq 1$. The worst-case input-output gain/phase margins m_g/m_ϕ are the highest value of the gain/phase shift that can be inserted without destabilizing the closed-loop. Δ_m and ω_m are the uncertainties and frequency, when this maximum gain/phase shift occurs.

Table 1. Performance metrics averaged on 50 simulations per patient (STD in parenthesis)

Patient ID	Time above range (%)		Time in range (%)	Time below range (%)	
	> 250(mg/dl)	180 – 250(mg/dl)	70 – 180(mg/dl)	54 – 70(mg/dl)	< 54(mg/dl)
1	0 (0)	13.25 (1.39)	86.75 (1.39)	0 (0)	0 (0)
2	0 (0)	8.95 (1.35)	91.05 (1.35)	0 (0)	0 (0)
3	0 (0)	9.02 (2.58)	90.98 (2.58)	0 (0)	0 (0)
4	0 (0)	11.94 (3.29)	88.06 (3.29)	0 (0)	0 (0)
5	0 (0)	26.23 (2.24)	73.77 (2.24)	0 (0)	0 (0)
6	0 (0)	24.50 (0.76)	75.50 (0.76)	0 (0)	0 (0)
7	0 (0.88)	22.14 (1.05)	77.86 (0.94)	0 (0.31)	0 (0)
8	0 (0)	33.52 (1.09)	66.48 (1.09)	0 (0)	0 (0)
9	0 (0)	18.04 (1.30)	81.96 (1.30)	0 (0)	0 (0)
10	0 (0)	4.58 (1.86)	95.42 (1.86)	0 (0)	0 (0)
11	0 (0)	20.6 (1.32)	79.94 (1.32)	0 (0)	0 (0)

In our case, the following results are obtained: $m_r \approx 1.1$ (highlighting robust stability for all considered patients, *i.e.* the unique designed controller is a stabilizing solution for the overall adults cohort), $m_g \approx 1.42$ (3dB), $m_\phi \approx 19^\circ$, $\omega_m \approx 0.0287$ rad/min and $\Delta_m = \text{diag}(1, -1)$. Since the worst-case gain shift occurs at the frequency ω_m where the uncertainties have been overestimated of approximately 1.5 dB (see Fig. 3), we argue that specification S.1 is met. Note that the worst-case uncertainties Δ_m corresponds to the patient $N^\circ 7$.

Worst-case analysis: Assuming that $m_r > 1$, one can compute the worst-case H_∞ performance level $m_\infty^{(S)}$ of S . $m_\infty^{(S)}$ is defined as the highest value of $\|\mathcal{F}_u(M, \Delta)\|_\infty$ when Δ takes its values in $\Delta : \|\Delta\|_\infty \leq 1$. $\omega_\infty^{(S)}$ is the frequency and $\Delta_\infty^{(S)}$ is the value of Δ when this worst-case happens. Similarly, $m_\infty^{(R)}$, $\omega_\infty^{(R)}$, $\Delta_\infty^{(R)}$ define the worst-case H_∞ performance criteria for the control sensitivity function $R(s, \Delta)$ defined in (15).

The frequency response of $S(s, \Delta)$ is plotted on Fig. 5. The maximum overshoot of $S(j\omega, \Delta)$ caused by the controller is $m_\infty^{(S)} \approx 3.37$ (10 dB) and happens at $\omega_\infty^{(S)} \approx 0.029$ rad/min for $\Delta_\infty^{(S)} = \text{diag}(1, -1)$. Since $\max_{\Delta \in \Delta : \|\Delta\|_\infty \leq 1} (\omega_c) < 0.03$ rad/min, we can conclude that (S.2) is met. In the same way, see Fig. 6, $m_\infty^{(R)} \approx 10.3$ (20 dB), $\omega_\infty^{(R)} \approx 0.033$ rad/min and $\Delta_\infty^{(R)} = \text{diag}(1, 1)$.

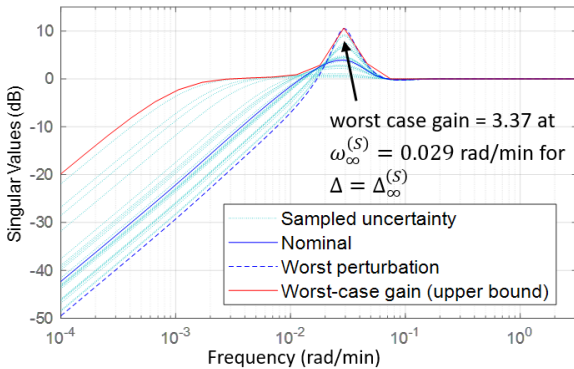


Fig. 5. Frequency response of $S(j\omega, \Delta)$

To conclude, the derived μ -criteria demonstrate that Specifications S.1) and S.2) are met.

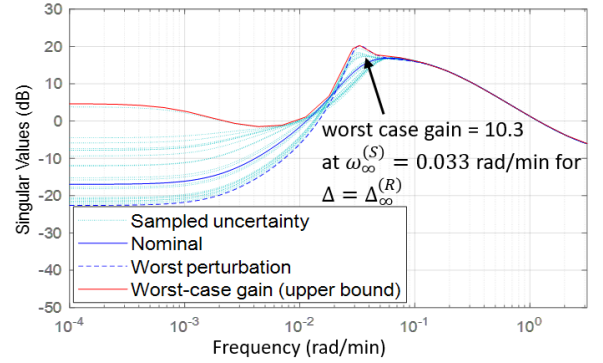


Fig. 6. Frequency response of $R(j\omega, \Delta)$

4. SIMULATION RESULTS

Using a Tustin approximation, the H_∞ controller is now implemented into the highly representative simulator UVA-Padova, with 11 virtual adult patients (possessing various and representative physiological parameters). It also includes a standard insulin pump as well as a standard CGM sensor (Breton and Kovatchev, 2008). The scenario consists of 3 announced meals: 60 g (of carbohydrate) at 7:00, 60 g, at 13:00 60 g and 60 g at 19:00. All meals have a duration of 15 min. The feedforward consists of a 2 U insulin bolus, delivered at the start of each meal (Steil et al., 2011). A total of 550 simulations (50 for each patients) are then run. The mean BG profile for all 550 simulations is plotted on Fig. 7 along with min/max envelopes and standard deviation. The minimal envelope is mainly caused by the patient $N^\circ 7$. It means that this patient is most prone to hypoglycemia risk, which is coherent with the analysis performed in section 3.4.

The results obtained are also analysed by means of clinical metrics, following the metrics advocated in (Battelino et al., 2019). These clinical specifications are mainly based on BG temporal distribution performance metrics, defined in terms of the so called “Time above/in/below range specification” metrics, in percentage, measured on one day. Table 2 gives values of these metrics.

The obtained results of our simulation campaign are listed in table 1. As it can be seen, no patient presents signs of hypoglycemia and only two patients associated metrics for hyperglycemia are over the recommended range: 1.2% over for patient $n^\circ 5$ and 8.5% over for patient $n^\circ 8$. These results validate to some extent the possibility of having a single controller for a patient’s cohort.

Table 2. Time in range specification

Metric	Specification
TAR ₂₅₀ (time above range > 250 mg/dL)	< 5%
TAR ₁₈₀ (time above range 181 – 250 mg/dL)	< 25%
TIR _{70–180} (time in range 70 – 180 mg/dL)	> 70%
TBR ₆₉ (time below range 54 – 69 mg/dL)	< 4%
TBR ₅₄ (time below range < 54 mg/dL)	< 1%

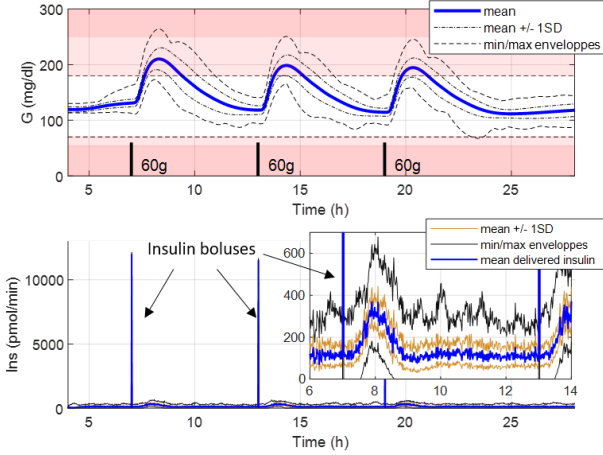


Fig. 7. Mean glucose profile for 550 simulations

5. CONCLUSION

Based on the H_∞/μ theory, this paper proposes the design of a robust controller in order to control the blood glucose profiles of type 1 Diabetes Mellitus patients. As opposed to existing commercial solutions, the solution is patient-independent and does not require either personalised tuning at feedback level or meal carbohydrate counting. The controller performance is assessed in the high fidelity UVA/Padova simulator, showing the potential of the proposed solution. Individualisation will be investigated in future works at feed-forward (meal announcement) or glucose target generation levels.

ACKNOWLEDGEMENTS

Research supported by the French National Agency for Research DIABLO ANR-18-CE17-0005-01, ECOSNord M18M01 and SEP-CONACYT-ECOS-ANUIES 296692.

REFERENCES

- Battelino, T., Danne, T., Bergenstal, R.M., et al. (2019). Clinical Targets for Continuous Glucose Monitoring Data Interpretation: Recommendations From the International Consensus on Time in Range. *Diabetes Care*, 42(8), 1593–1603.
- Breton, M. and Kovatchev, B. (2008). Analysis, Modeling, and Simulation of the Accuracy of Continuous Glucose Sensors. *Journal of Diabetes Science and Technology*, 2(5), 853–862.
- Cassany, L., Gucik-Derigny, D., Cieslak, J., et al. (2021). A Robust Control solution for Glycaemia Regulation of Type-1 Diabetes Mellitus. In *IEEE European Control Conference*. Rotterdam, Netherlands.
- Colmegna, P.H., Bianchi, F.D., and Sánchez-Peña, R.S. (2021). Automatic Glucose Control During Meals and Exercise in Type 1 Diabetes: Proof-of-Concept in Silico Tests Using a Switched LPV Approach. *IEEE Control Systems Letters*, 5(5), 1489–1494.
- Dalla Man, C., Micheletto, F., Lv, D., et al. (2014). The UVA/PADOVA Type 1 Diabetes Simulator: New Features. *Journal of Diabetes Science and Technology*, 8(1), 26–34.
- Del Favero, S., Bruttomesso, D., Di Palma, F., et al. (2014). First Use of Model Predictive Control in Outpatient Wearable Artificial Pancreas. *Diabetes Care*, 37(5), 1212–1215.
- Femat, R., Ruiz-Velazquez, E., and Quiroz, G. (2009). Weighting Restriction for Intravenous Insulin Delivery on T1DM Patient via H_∞ Control. *IEEE Transactions on Automation Science and Engineering*, 6(2), 239–247.
- Flores-Gutiérrez, C., Femat, R., and Ruiz-Velázquez, E. (2011). On hypoglycemic levels induced by H_∞ control on type I diabetes mellitus. *Applied Math. and Comp.*, 218(2), 376–385.
- Franco, R., Ferreira de Loza, A., Ríos, H., Cassany, L., et al. (2021). Output-Feedback Sliding-Mode Controller for Blood Glucose Regulation in Critically Ill Patients Affected by Type 1 Diabetes. *IEEE Transactions on Control Systems Technology*, 1–8.
- Gahinet, P. and Apkarian, P. (1994). A linear matrix inequality approach to h_∞ control. *International Journal of Robust and Nonlinear Control*, 4(4), 421–448.
- Gallardo Hernández, A.G., Fridman, L., Levant, A., et al. (2013). High-order sliding-mode control for blood glucose: Practical relative degree approach. *Control Engineering Practice*, 21(5), 747–758.
- Gondhalekar, R., Dassau, E., and Doyle, F.J. (2018). Velocity-weighting & velocity-penalty MPC of an artificial pancreas: Improved safety & performance. *Automatica*, 91, 105–117.
- Hernández-Medina, A., Flores-Gutiérrez, C., and Femat, R. (2018). Robustness properties preservation in suboptimal T1DM H_∞ control: ω -SPR substitutions. *Optimal Control Applications and Methods*, 39(1), 220–229.
- Kienitz, K.H. and Yoneyama, T. (1993). A robust controller for insulin pumps based on H-infinity theory. *IEEE transactions on bio-medical engineering*, 40(11), 1133–1137.
- Kovács, L. (2017). Linear parameter varying (lpv) based robust control of type-1 diabetes driven for real patient data. *Knowledge-Based Systems*, 122, 199–213.
- Kwakernaak, H. (1993). Robust control and H_∞ -optimization—Tutorial paper. *Automatica*, 29(2), 255–273.
- Mandal, S., Bhattacharjee, A., and Sutradhar, A. (2014). LMI Based Robust Blood Glucose Regulation in Type-1 Diabetes Patient with Daily Multi-meal Ingestion. *Journal of The Institution of Engineers (India): Series B*, 95(2), 121–128.
- Messori, M., Paolo Incremona, G., Cobelli, C., et al. (2018). Individualized model predictive control for the artificial pancreas: In silico evaluation of closed-loop glucose control. *IEEE Control Systems Magazine*, 38(1), 86–104.
- Olcomendy, L., Pirog, A., Bornat, Y., et al. (2020). Tuning of an Artificial Pancreas Controller: an in silico methodology based on clinically-relevant criteria *. In *2020 42nd Annual International Conference of the IEEE Engineering in Medicine & Biology Society (EMBC)*, 2544–2547. IEEE.
- Packard, A. and Doyle, J. (1993). The complex structured singular value. *Automatica*, 29(1), 71–109.
- Parker, R.S., Doyle, F.J., Ward, J.H., et al. (2000). Robust H_∞ glucose control in diabetes using a physiological model. *AICHE Journal*, 46(12), 2537–2549.
- Quiroz, G. (2019). The evolution of control algorithms in artificial pancreas: A historical perspective. *Annual Reviews in Control*, 48, 222–232.
- Rodbard, D. (2016). Continuous Glucose Monitoring: A Review of Successes, Challenges, and Opportunities. *Diabetes Technology & Therapeutics*, 18(S2), S2–3–S2–13.
- Ruiz-Velázquez, E., Femat, R., and Campos-Delgado, D. (2004). Blood glucose control for type I diabetes mellitus: A robust tracking H_∞ problem. *Control Engineering Practice*, 12(9), 1179–1195.
- Steil, G.M., Palerm, C.C., Kurtz, N., et al. (2011). The Effect of Insulin Feedback on Closed Loop Glucose Control. *The Journal of Clinical Endocrinology & Metabolism*, 96(5), 1402–1408.
- Zhou, K. and Doyle, J.C. (1998). *Essentials of robust control*. Prentice Hall, Upper Saddle River, N.J.